SOILS AND FOUNDATIONS Vol. 47, No. 4, 635–648, Aug. 2007
Japanese Geotechnical Society

# EXPLANATION OF CYCLIC MOBILITY OF SOILS: APPROACH BY STRESS-INDUCED ANISOTROPY

FENG ZHANG[i], BIN YE[ii], TOSHIHIRO NODA[iii], MASAKI NAKANO[iv] and KENTARO NAKAI[v]

## ABSTRACT

In this paper, a new constitutive model is proposed to describe the mechanical behaviors of soils under different loading conditions. New evolution equations for the development of stress-induced anisotropy and the change of overconsolidation of soils are proposed. By combining systematically the above two evolution equations with the evolution equation for the structure of soil proposed by Asaoka et al. (2002), the newly proposed model is able to describe not only the mechanical behavior of soils under monotonic loading, but also the behavior of soils under cyclic loading with different drained condition. Special attention is paid to the behavior of sand subjected to cyclic loading under undrained condition. That is, for given sand with different densities, very loose sand may liquefy without cyclic mobility, medium dense sand will liquefy with cyclic mobility while dense sand will not liquefy, which is just controlled by the density, the structure and the anisotropy of the sand. A suitable model should uniquely describe this behavior without changing its parameters. Present research will show the possibility of the proposed model.

**Key words:** anisotropy, constitutive model, cyclic mobility, over consolidation, structure (**IGC**: D6)

## INTRODUCTION

Much research has been done on the liquefaction of soils experimentally, empirically, and mathematically. In many cases, the researchers could not avoid addressing the topic of ''the cyclic mobility of soils'' in their studies. This is because if we want to know the mechanical behavior of soils during liquefaction at the element level, we must conduct undrained shear tests under cyclic loading, e.g., triaxial tests and hollow-cylinder shear tests. In doing so, the capability of a research work to deal with the cyclic mobility of soils becomes a key factor. Research related to the testing methods and the modeling of the cyclic mobility of soils can be found in many publications. For instance, in the works by Oka et al. (1992, 1999), a constitutive model for sand, using the kinematic hardening rule, was proposed and then applied to the boundary value problem (BVP) by a soil-water coupling finite element-finite difference analysis with the LIQCA program (Yashima et al., 1991; Oka et al., 1994). Oka (1992) also proposed an elasto-viscoplastic model for clay using the kinematic hardening rule. The aforementioned works introduced approaches for describing the mechanical behavior of soils subjected to cyclic loading under undrained conditions, and based them on first being able to solve the BVP for the liquefaction of soils with a strict soil-water two-phase field theory. Many other studies related to this field have been conducted, but we are unable to list them all at this time.

In recent years, research on constitutive model for soils has been developing very quickly. Some works in particular are worthy of mention in advance. The term ''initial anisotropy'' was firstly proposed to describe the phenomenon of anisotropy by Sekiguchi (1977), although the author did not use this term in the beginning. Then, Hashiguchi and Chen (1998) proposed a rotation tensor to describe stress-induced anisotropy. The concept of ''subloading'' was proposed by Hashiguchi and Ueno (1977), Hashiguchi (1978, 1989), which made it possible to describe the overconsolidation of soils easily and efficiently. The concept of ''superloading'', proposed by Asaoka et al. (1998), Asaoka et al. (2000a), and Asaoka et al. (2000b), together with the concept of subloading, make it possible not only to describe overconsolidation, but also to explain the effect of the soil structure commonly observed in naturally deposited soils, which is one of the main reasons why soils may differ greatly from place to place. By combining the concepts of subloading and superloading, it is possible for the first time to describe the mechanical behavior of clay and sand with different densities and different structures within the same framework of a constitutive model. The proposed model

[i] Professor, Department of Civil Engineering, Nagoya Institute of Technology, Nagoya, Japan (zhang-f@tutil.ace.nitech.ac.jp).
[ii] Graduate Student, Department of Civil Engineering, Gifu University, Gifu, Japan.
[iii] Associate Professor, Department of Civil Engineering, Nagoya University, Nagoya, Japan.
[iv] Associate Professor, ditto.
[v] Research Associate, ditto.
The manuscript for this paper was received for review on March 9, 2006; approved on March 26, 2007.
Written discussions on this paper should be submitted before March 1, 2008 to the Japanese Geotechnical Society, 4-38-2, Sengoku, Bunkyo-ku, Tokyo 112-0011, Japan. Upon request the closing date may be extended one month.

is based on the Cam-clay model (Roscoe et al., 1963) and the modified Cam-clay model (Schofield and Wroth, 1968). Therefore, the physical meaning of the model is easy to understand and relatively few parameters need to be employed in spite of its ability to deal with different soils using the same model.

Asaoka et al. (2002) proposed an elasto-plastic constitutive model for soils, based on the evolution rules which describe the collapse of the soil skeleton structure (the concept of superloading), the loss in overconsolidation (the concept of subloading), and the development of anisotropy during shearing. In their paper, the importance of stress-induced anisotropy is introduced. It is found from this research that the liquefaction of loose sand can be described by the collapse of the soil skeleton structure. The cyclic mobility of medium dense sand, however, could not be described accurately at first by the collapse of the soil skeleton structure. It has been found in recent research that by introducing the concept of ''regaining the structure during shearing'', the possibility of describing the cyclic mobility of medium dense sand is confirmed. These results will be published soon by the same authors.

In this paper, contrary to the approach of ''the collapse of the structure'', the authors propose a new approach for describing the stress-induced anisotropy together with a new evolution rule for changes in overconsolidation, by which the mechanical behavior of soils subjected to cyclic loading under undrained conditions, including the cyclic mobility of medium dense sand, can be uniquely described. Meanwhile, the physical meaning of these types of behavior for different soils can be explained efficiently with the concepts of overconsolidation, structure, and stress-induced anisotropy.

## MODELING OF CYCLIC MOBILITY

The model proposed here, is based on the concepts of subloading and superloading as described in the work by Asaoka et al. (2002). Here we give just a brief description of the yielding surfaces shown in Fig. 1.

The similarity ratio of the superloading surface to normal yield surface $R^*$ and the similarity ratio of the superloading surface to subloading surface $R$ are the same as

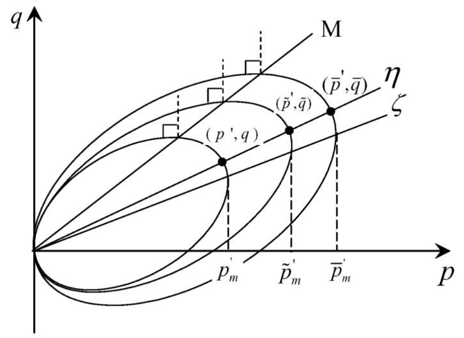


**Fig. 1. Subloading, normal and superloading yield surfaces in *p-q* plane adopted in the present model**

those in the work by Asaoka et al. (2002), namely,

$$R^* = \frac{\tilde p'}{\bar p'} = \frac{\tilde q}{\bar q},\ 0 < R^* \le 1 \text{ and } \frac{\tilde q}{\tilde p'} = \frac{\bar q}{\bar p'} \tag{1}$$

$$R = \frac{p'}{\bar p'} = \frac{q}{\bar q},\ 0 < R \le 1, \text{ and } \frac{\bar q}{\bar p'} = \frac{\tilde q}{\tilde p'} = \frac{q}{p'} \tag{2}$$

where, $(p', q)$, $(\tilde p', \tilde q)$ and $(\bar p', \bar q)$ represent the present stress state, the corresponding normally consolidated stress state and the structured stress state at *p-q* plane, respectively. The normally yield surface is given in the following form as:

$$f(\tilde p', \tilde\eta^*, \zeta) + \int_0^t J \mathrm{tr} \boldsymbol{D}^p d\tau =$$

$$\mathrm{MD} \ln \frac{\tilde p'}{\tilde p'_0} + \mathrm{MD} \ln \frac{\mathrm{M}^2 - \zeta^2 + \tilde\eta^{*2}}{\mathrm{M}^2 - \zeta^2} + \int_0^t J \mathrm{tr} \boldsymbol{D}^p d\tau = 0 \tag{3}$$

where, $\tilde\eta^* = \eta^*$, and the other variables involved in Eq. (1), (2) and (3) are defined as:

$$\eta^* = \sqrt{\frac{3}{2} \hat{\boldsymbol{\eta}} \cdot \hat{\boldsymbol{\eta}}}, \quad \hat{\boldsymbol{\eta}} = \boldsymbol{\eta} - \boldsymbol{\beta}, \quad \boldsymbol{\eta} = \frac{\boldsymbol{S}}{p'},$$

$$\boldsymbol{S} = \boldsymbol{T}' + p'\boldsymbol{I}, \quad p' = -\frac{1}{3} \mathrm{tr} \boldsymbol{T}' \tag{4}$$

$$\zeta = \sqrt{\frac{3}{2} \boldsymbol{\beta} \cdot \boldsymbol{\beta}}, \quad \eta = \sqrt{\frac{3}{2} \boldsymbol{\eta} \cdot \boldsymbol{\eta}} \tag{5}$$

where, $\boldsymbol{S}$ is the deviatoric stress tensor; $\boldsymbol{\beta}$ is the anisotropic stress tensor, and $\boldsymbol{T}'$ is the Cauchy effective stress tensor and is assumed to be positive in tension. The definition for the surface is different from the previous one in its critical state line (C.S.L.). In the previous definition, the C.S.L. (the border line distinguishing dilation and compression) is defined by the $\mathrm{M}_a$ ($\mathrm{M}_a^2 = \mathrm{M}^2 + \zeta^2$), in which $\zeta$ is the magnitude of the stress-induced anisotropy. It is clear that the gradient of the C.S.L .changes with the development of anisotropy. It will be shown later that the gradient of the C.S.L. for the present model is constant. The physical evidence of fixing the gradient of the C.S.L. can be found in many literatures, e.g., the work by Hyodo et al. (1994) and Kato et al. (2001). It is also very clear from both the definition and Fig. 2 that the flat ratio of the elliptical yield surface changes with the value of anisotropy. The larger the stress-induced anisotropy $\zeta$ is, the larger the eccentric ratio of the ellipse will be. In Eq. (3), $J$ is the Jacobian determination of deformation gradient tensor $\boldsymbol{F}$ and can be expressed as:

$$J = \det \boldsymbol{F} = \frac{\mathrm{v}}{\mathrm{v}_0} = \frac{1+e}{1+e_0} \tag{6}$$

where v and $\mathrm{v}_0$ are the specific volume at the current time ($t$) and the specific value at the reference time ($t=0$). D is the dilatancy parameter which can be expressed by $\tilde\lambda$, $\tilde\kappa$, the compression and the swelling index, respectively, as follows:

$$\mathrm{D} = \frac{\tilde\lambda - \tilde\kappa}{\mathrm{M}(1+e_0)} = \frac{\tilde\lambda - \tilde\kappa}{\mathrm{M}\mathrm{v}_0} \tag{7}$$

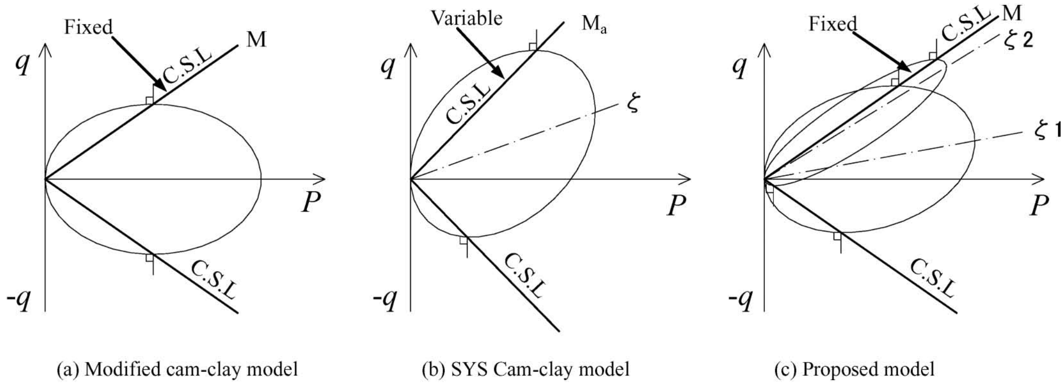


(a) Modified cam-clay model (b) SYS Cam-clay model (c) Proposed model

**Fig. 2. Changes in the subloading yielding surfaces at different anisotropy $\zeta$**

$\boldsymbol{D}^p$ denotes the plastic component of stretching $\boldsymbol{D}$ which is assumed to be positive in tension, and is related to the plastic volumetric strain rate in the following form under the condition that the compressive of the volumetric strain is supposed to be positive:

$$\varepsilon_v^p = -\int_0^t J\mathrm{tr}\boldsymbol{D}^p d\tau \tag{8}$$

By substituting Eq. (1) and (2) into Eq. (3), the subloading yield surface can be obtained in the following equation as:

$$\begin{aligned} f(p', \eta^*, \zeta) + \mathrm{MD}\ln R^* - \mathrm{MD}\ln R + \int_0^t J\mathrm{tr}\boldsymbol{D}^p d\tau \quad (9)\\ = \mathrm{MD}\ln\frac{p'}{p'_0} + \mathrm{MD}\ln\frac{\mathrm{M}^2-\zeta^2+\eta^{*2}}{\mathrm{M}^2-\zeta^2} + \mathrm{MD}\ln R^* \\ - \mathrm{MD}\ln R + \int_0^t J\mathrm{tr}\boldsymbol{D}^p d\tau = 0 \end{aligned}$$

Figure 3 shows the changes in the subloading yielding surface in the cyclic mobility stage, from which it is clear that not only the size of the surface but also the axis of elliptical yield surface change according to the states of present stress and the stress-induced anisotropy.

An associated flow rule is employed in the present model, namely,

$$\boldsymbol{D}^p = \lambda\frac{\partial f}{\partial \boldsymbol{T}'} \tag{10}$$

The consistency equation for the subloading yield surface can then be given as:

$$\frac{\partial f}{\partial \boldsymbol{T}'}\cdot\mathring{\boldsymbol{T}}' + \frac{\partial f}{\partial \boldsymbol{\beta}}\cdot\mathring{\boldsymbol{\beta}} + \mathrm{MD}\frac{\dot{R}^*}{R} - \mathrm{MD}\frac{\dot{R}}{R^*} + J\mathrm{tr}\boldsymbol{D}^p = 0 \tag{11}$$

where

$$\mathring{\boldsymbol{T}}' = \dot{\boldsymbol{T}}' + \boldsymbol{T}'\boldsymbol{\Omega} = \boldsymbol{\Omega}\boldsymbol{T}',\ \mathring{\boldsymbol{\beta}} = \dot{\boldsymbol{\beta}} + \boldsymbol{\beta}\boldsymbol{\Omega} - \boldsymbol{\Omega}\boldsymbol{\beta} \tag{12}$$

in which, $\mathring{\boldsymbol{T}}'$ and $\mathring{\boldsymbol{\beta}}$ are the Green-Naghdi rates (1965) of stress tensor $\boldsymbol{T}'$ and anisotropic stress tensor $\boldsymbol{\beta}$, respectively. $\boldsymbol{\Omega}$ is material spin tensor. The following differentials are useful in deriving the constitutive equation for the stress tensor and the stretching tensor:

$$\frac{\partial(\eta^{*2})}{\eta p'} = -\frac{3\hat{\boldsymbol{\eta}}\cdot\boldsymbol{\eta}}{p'},\ \frac{\partial(\eta^{*2})}{\partial \boldsymbol{S}} = \frac{3\hat{\boldsymbol{\eta}}}{p'} \tag{13}$$

$$\frac{\partial(\eta^{*2})}{\partial\boldsymbol{\beta}} = -3\hat{\boldsymbol{\eta}},\ \frac{\partial(\zeta^2)}{\partial\boldsymbol{\beta}} = 3\boldsymbol{\beta} \tag{14}$$

Based on Eq. (13) and (14), it is easy to obtain the following relations:

$$\frac{\partial f}{\partial p'} = \mathrm{MD}\left(\frac{1}{p'} + \frac{\dfrac{\partial(\eta^{*2})}{\partial p'}}{\mathrm{M}^2-\zeta^2+\eta^{*2}}\right) = \mathrm{MD}\frac{\mathrm{M}^2-\eta^2}{(\mathrm{M}^2-\zeta^2+\eta^{*2})p'} \tag{15}$$

$$\frac{\partial f}{\partial \boldsymbol{S}} = \mathrm{MD}\frac{3\hat{\boldsymbol{\eta}}}{(\mathrm{M}^2-\zeta^2+\eta^{*2})p'} \tag{16}$$

$$\begin{aligned}\frac{\partial f}{\partial \boldsymbol{T}'} = \frac{\partial f}{\partial \boldsymbol{S}} + \frac{1}{3}\frac{\partial f}{\partial p'}\boldsymbol{I} = \mathrm{MD}\Bigg(\frac{3\hat{\boldsymbol{\eta}}}{(\mathrm{M}^2-\zeta^2+\eta^{*2})p'} \\ + \frac{1}{3}\frac{\mathrm{M}^2-\eta^2}{(\mathrm{M}^2-\zeta^2+\eta^{*2})p'}\boldsymbol{I}\Bigg)\end{aligned} \tag{17}$$

$$\begin{aligned}\frac{\partial f}{\partial\boldsymbol{\beta}} &= \mathrm{MD}\left(\frac{-\dfrac{\partial(\zeta^2)}{\partial\boldsymbol{\beta}} + \dfrac{\partial(\eta^{*2})}{\partial\boldsymbol{\beta}}}{\mathrm{M}^2-\zeta^2+\eta^{*2}} - \frac{-\dfrac{\partial(\zeta^2)}{\partial\boldsymbol{\beta}}}{\mathrm{M}^2-\zeta^2}\right) \\ &= \mathrm{MD}\frac{3(-\mathrm{M}^2\hat{\boldsymbol{\eta}} + \eta^{*2}\boldsymbol{\beta} + \zeta^2\hat{\boldsymbol{\eta}})}{(\mathrm{M}^2-\zeta^2+\eta^{*2})(\mathrm{M}^2-\zeta^2)}\end{aligned} \tag{18}$$

From Eq. (15), it is clear that the C.S.L., defined by the condition in which $\partial f/\partial p' = 0$, always satisfies the relation $\eta = \mathrm{M}$, implying that the C.S.L., as the threshold between plastic compression and plastic expansion, does not move with the changes in the anisotropy.

*Evolution Rule for Stress-induced Anisotropic Stress Tensor $\boldsymbol{\beta}$*

Different from the work by Hashiguchi and Chen (1998) and Asaoka et al. (2002), the following evolution rule for the anisotropic stress tensor is defined as:

$$\mathring{\boldsymbol{\beta}} = \frac{J}{\mathrm{D}}b_r(b_l\mathrm{M} - \zeta)\sqrt{\frac{3}{2}}\left\|\boldsymbol{D}_s^p\right\|\frac{\hat{\boldsymbol{\eta}}}{\|\hat{\boldsymbol{\eta}}\|} \tag{19}$$

in which, an artificial limitation on the development of anisotropy originally proposed by Hashiguchi and Chen

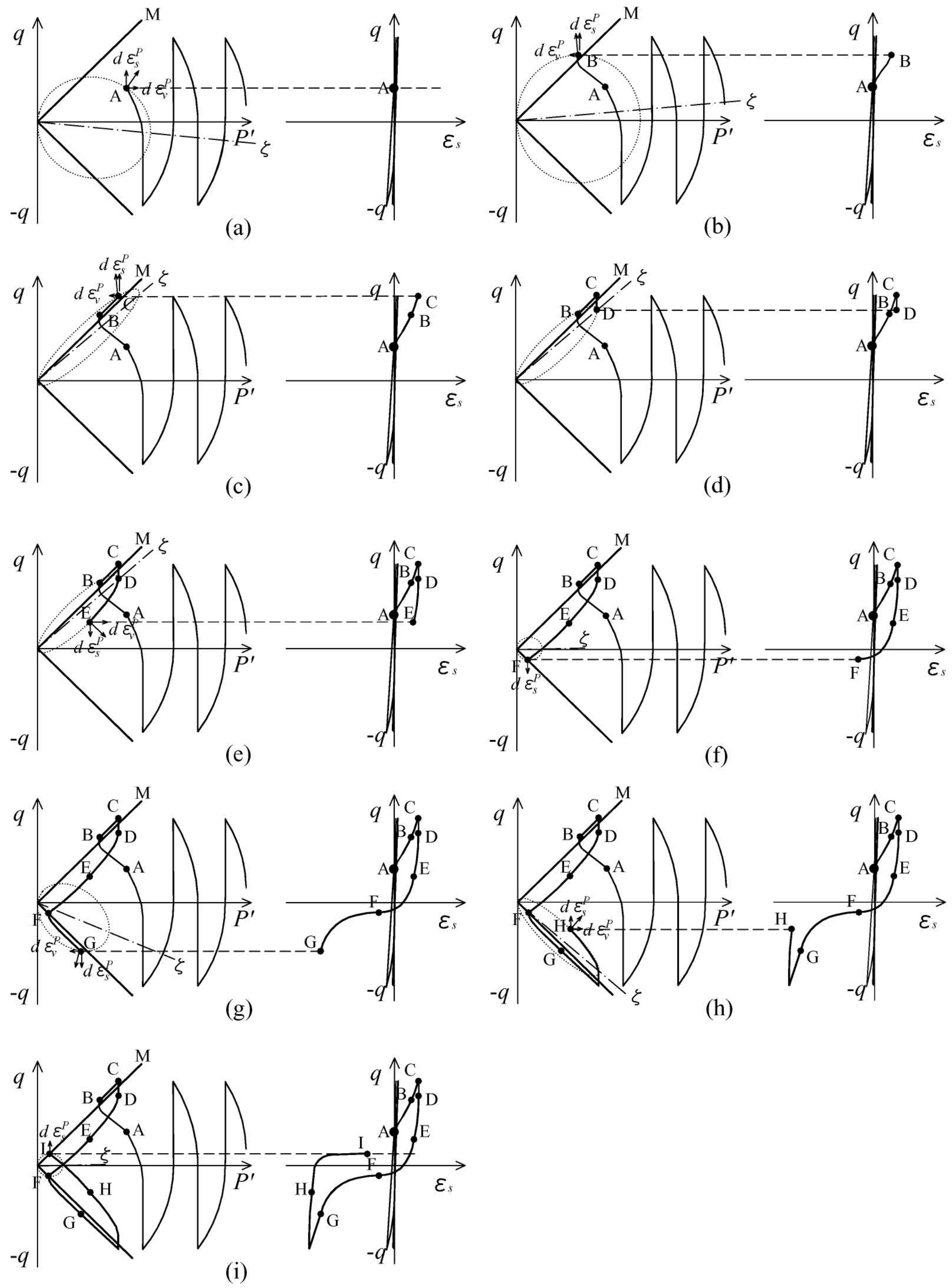

**Fig. 3. Changes in the subloading yielding surface in the cyclic mobility stage**

(1998) is no longer necessary, because firstly it more or less lacks physical evidence and secondly the stress-induced anisotropic stress tensor $\boldsymbol{\beta}$ also represents the stress history that the soil experienced and it will not exceed the C.S.L., which provides us with a natural physical limitation $\zeta < M$, that can be easily accepted. In order to avoid the singularity in Eq. (3) at the point $\zeta = M$, a limitation parameter $b_l$ in Eq. (19) is introduced. Its value varies from 0.90 to 0.99 according to the explanation of 'completely liquefaction' in an engineering sense. The closer the value of $b_l$ is to 1.0, the closer the mean effective stress will be to zero in the cyclic mobility region. Without losing physical meaning, we fixed the value of $b_l$ at 0.95 throughout this paper. From the evolution Eq. (19), it is also known that development of anisotropy will stop at the state when. $\boldsymbol{\eta} = \boldsymbol{\beta}$.

Author may ask a question that when using a plastic potential of modified Cam-clay type, the effective stress path may not move along a strait line ($\eta_0$-line) under $K_o$ consolidation. It is true and it is not only for the modified Cam-clay type but also for any other plastic model. Remember that $K_o$ consolidation is conducted under the condition that the lateral deformation is restricted. It is a given-displacement boundary value problem (BVD).

Therefore, theoretically, the stress path has never been assigned! In engineering, however, some geotechnical engineers regard that in $K_o$ consolidation, the stress path moves along the $\eta_0$-line, which is a proximate result and not a strict discipline.

The plastic component of stretching tensor $\boldsymbol{D}_s^p$ can be calculated as follow:

$$\boldsymbol{D}_s^p = \boldsymbol{D}^p - \frac{1}{3}(\mathrm{tr}\boldsymbol{D}^p)\boldsymbol{I} = \lambda\frac{\partial f}{\partial \boldsymbol{S}} \tag{20}$$

$$\|\boldsymbol{D}_s^p\| = \lambda\sqrt{\frac{\partial f}{\partial \boldsymbol{S}}\cdot\frac{\partial f}{\partial \boldsymbol{S}}} = \lambda \mathrm{MD}\frac{3\|\hat{\boldsymbol{\eta}}\|}{(\mathrm{M}^2 - \zeta^2 + \eta^{*2})p'} \tag{21}$$

Substituting Eq. (21) into Eq. (19), the evolution rule for the anisotropic stress tensor can be rewritten as:

$$\overset{\circ}{\boldsymbol{\beta}} = \lambda\frac{J\mathrm{M}\sqrt{6}\,b_r(b_l\mathrm{M} - \zeta)\hat{\boldsymbol{\eta}}}{(\mathrm{M}^2 - \zeta^2 + \eta^{*2})p'} \tag{22}$$

Applying Eq. (18) and (22), it is easy to calculate the increment in anisotropy as follows:

$$\frac{\partial f}{\partial \boldsymbol{\beta}}\cdot\overset{\circ}{\boldsymbol{\beta}} = \lambda \mathrm{MD}\frac{J\mathrm{M}\sqrt{6}\,b_r(b_l\mathrm{M} - \zeta)\eta^{*2}(-2\mathrm{M}^2 + 3\boldsymbol{\eta}\cdot\boldsymbol{\beta})}{(\mathrm{M}^2 - \zeta^2 + \eta^{*2})^2(\mathrm{M}^2 - \zeta^2)p'} \tag{23}$$

which plays a very important role in the evolution rule for the overconsolidation that will be discussed later. From Eq. (23), it is clear that if $\boldsymbol{\eta}\cdot\boldsymbol{\beta} \le 0$, which means the angle between the deviatoric stress tensor and the anisotropic tensor is larger than 90°, then $(\partial f/\partial \boldsymbol{\beta})\cdot\overset{\circ}{\boldsymbol{\beta}}$ will always be less than zero.

*Evolution rule for degree of structure $R^*$*

The following evolution rule for degree of structure $R^*$, which is the same as in the work by Asaoka et al. (2002), is adopted:

$$\dot{R}^* = JU^*\sqrt{\frac{2}{3}}\|\boldsymbol{D}_s^p\| \tag{24}$$

where,

$$U^* = \frac{a}{\mathrm{D}}R^*(1 - R^*) \quad (0 < R^* \le 1) \tag{25}$$

in which a is the parameter that controls the rate of the collapse of the structure during shearing. From the definition, it is clear that the structure of a soil will never be regained once it has been lost. This seems natural because, based on the physical process, the structure of a soil is accumulated during the sedimentary process over a long period time and it would not be easy to regain it within a short period of time without any chemical processes. Substituting Eq. (21) and (25) into Eq. (24), the rate of $R^*$ can be evaluated as:

$$\dot{R}^* = \lambda\frac{J\mathrm{M}aR^*(1 - R^*)\eta^*}{(\mathrm{M}^2 - \zeta^2 + \eta^{*2})p'} \tag{26}$$

*Evolution Rule for Degree of Overconsolidation $R$*

In the present model, the changing rate of overconsolidation is assumed to be controlled by two factors, namely, the plastic component of stretching that was employed as the only factor in the work by Asaoka et al. (2002), and the increment in anisotropy, in other words,

$$\dot{R} = JU\|\boldsymbol{D}^p\| + \frac{R}{\mathrm{MD}}\frac{\eta}{\mathrm{M}}\frac{\partial f}{\partial \boldsymbol{\beta}}\cdot\overset{\circ}{\boldsymbol{\beta}} \tag{27}$$

In which, by the definition of $\overset{\circ}{\boldsymbol{\beta}}$ in Eq. (19), $\overset{\circ}{\boldsymbol{\beta}}$ is proportional to the norm of the plastic component of stretching $\|\boldsymbol{D}_s^p\|$. Therefore Eq. (27) is a strict evolution rule for the degree of overconsolidation. $U$ is given by the following relation as:

$$U = -\frac{m}{\mathrm{D}}\left(\frac{p'}{p_0'}\right)^2 \ln R$$

$$(p_0' = 98.0\ \mathrm{kPa,\ reference\ stress}) \tag{28}$$

The purpose of adding $(p'/p_0')^2$ into the first term in Eq. (27) is to keep the $U$ as small as possible when $p'$ is very small, so that the stress may be maintained in highly overconsolidated state for as long as possible. As a result, in Step (I) shown in both Fig. 3 and 4 where only the plastic shear strain component is developing (no plastic volumetric strain has developed), the shear strain developed very quickly while the stress remains unmoved. The second part of Eq. (27) is adopted to assure the quick acquisition of overconsolidation (a reduction in $R$) in the period from (H) to (I) shown in Fig. 4. It is clear from Eq. (27) that, apart from elastic unloading, the acquisition of overconsolidation (a reduction in $R$) is impossible in the plastic loading process if only the first part of Eq. (27) is used, as in the works by Asaoka et al. (2002). Therefore, it is understood from Fig. 4 (b), the change of anisotropic stress difference with mean effective stress, that the first term in Eq. (27) functions well in regions far from the cyclic loading region, while the second term in Eq. (27) functions well within the cyclic loading region. Without introducing the second term, it is impossible to accumulate overconsolidation, and therefore, impossible to describe the cyclic mobility. The reason for this is that the second term in Eq. (27) has a strict mathematical meaning. In the process from Step (H) to Step (I) shown in Figs. 4(a) and (d), $R$ changes very quickly while the effective stress does not move at all (*see* Fig. 3(I)); the plastic volumetric strain rate is exactly zero, and the degree of structure is almost one. By substituting the above conditions into Eq. (11), we can immediately obtain the formula for the second term in Eq. (27). From Eq. (23), we can also see that if the angle between the deviatoric stress tensor and the anisotropic tensor is larger than 90°, then $\boldsymbol{\eta}\cdot\boldsymbol{\beta} \le 0$; therefore, $(\partial f/\partial \boldsymbol{\beta})\cdot\overset{\circ}{\boldsymbol{\beta}}$ will always be less than zero. This implies that the overconsolidation is accumulated during the plastic loading process. The reason for using the term $(p'/p_0')^2$ is that in the region close to zero, the effective stress is very small and the change of the effective stress is also very slow compared with the quick development of plastic strain. Therefore it is necessary to slow down the changing rate of overconsolidation, that is, to let $U$ be a small value.

Using Eqs. (10) and (17), it is easy to obtain the relation as

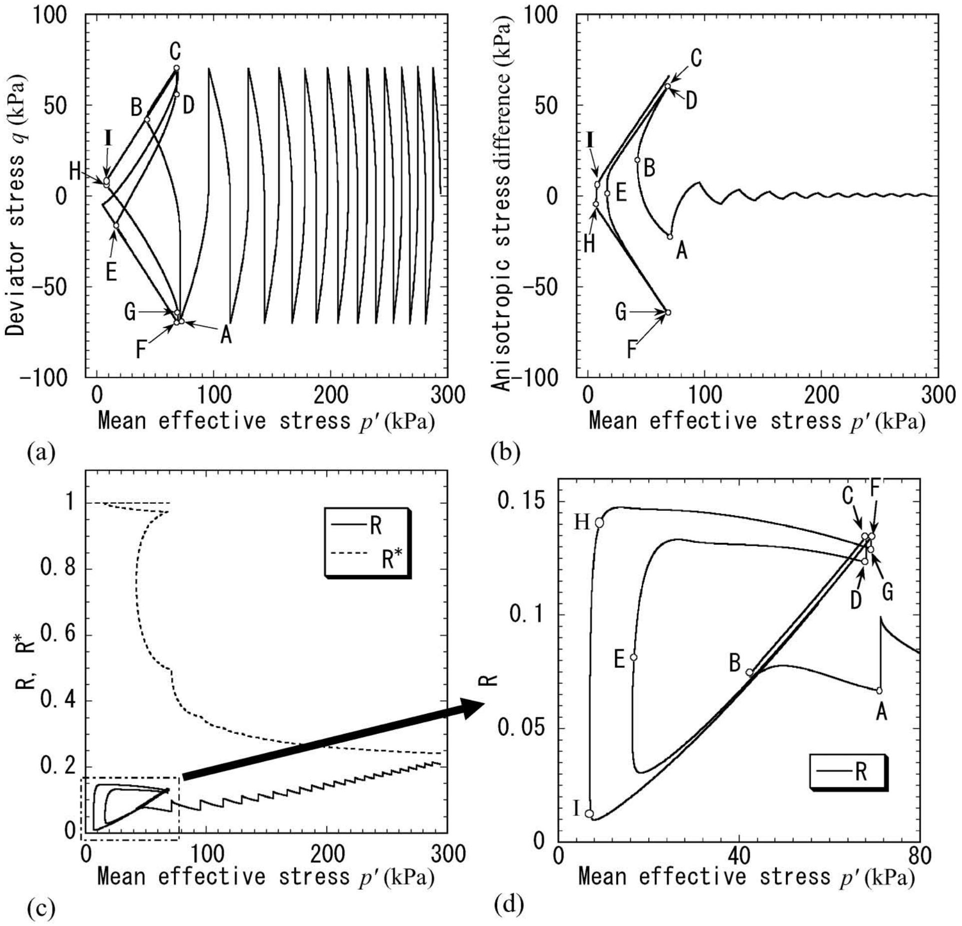


**Fig. 4. Changes in $R$, $R^*$, and $\zeta$ in or away from the cyclic mobility region**

$$\|\boldsymbol{D}^p\| = \sqrt{\boldsymbol{D}^p \cdot \boldsymbol{D}^p} = \lambda \mathrm{MD} \frac{\sqrt{6\eta^{*2} + \dfrac{1}{3}(\mathrm{M}^2 - \eta^2)^2}}{(\mathrm{M}^2 - \zeta^2 + \eta^{*2})p'} \tag{29}$$

Substituting Eqs. (28) and (29) into Eq. (27), we obtain:

$$\dot{R} = \lambda \frac{-mJ\mathrm{M} \ln R \sqrt{6\eta^{*2} + \dfrac{1}{3}(\mathrm{M}^2 - \eta^2)^2}}{(\mathrm{M}^2 - \zeta^2 + \eta^{*2})p'} \left(\frac{p'}{p'_0}\right)^2 + \frac{R}{\mathrm{MD}} \frac{\eta}{\mathrm{M}} \frac{\partial f}{\partial \boldsymbol{\beta}} \cdot \mathring{\boldsymbol{\beta}} \tag{30}$$

The plastic volumetric strain rate can be evaluated as:

$$-\dot{\varepsilon}_v^p = J\mathrm{tr}\boldsymbol{D}^p = J\lambda \mathrm{tr}\frac{\partial f}{\partial \boldsymbol{T}'} = J\mathrm{MD}\lambda \frac{\mathrm{M}^2 - \eta^2}{(\mathrm{M}^2 - \zeta^2 + \eta^{*2})p'} \tag{31}$$

Substituting Eqs. (23), (26), (30) and (31) into Eq. (11), the positive valuable $\lambda$ can then be determined as:

$$\lambda = \frac{\dfrac{\partial f}{\partial \boldsymbol{T}'} \cdot \mathring{\boldsymbol{T}}'}{J \dfrac{\mathrm{MD}}{(\mathrm{M}^2 - \zeta^2 + \eta^{*2})p'} (\mathrm{M}_s^2 - \eta^2)} \tag{32}$$

where

$$\mathrm{M}_s^2 = \mathrm{M}^2 - \frac{m\mathrm{M} \ln R}{R} \left(\frac{p'}{p'_0}\right) \sqrt{6\eta^{*2} + \frac{1}{3}(\mathrm{M}^2 - \eta^2)^2} - 2a\mathrm{M}(1 - R^*)\eta^* + \left(1 - \frac{\eta}{\mathrm{M}}\right) \frac{\sqrt{6}\,\mathrm{M}b_r(b_l\mathrm{M} - \zeta)\eta^{*2}(2\mathrm{M}^2 - 3\boldsymbol{\eta} \cdot \boldsymbol{\beta})}{(\mathrm{M}^2 - \zeta^2 + \eta^{*2})(\mathrm{M}^2 - \zeta^2)} \tag{33}$$

If the stretching is divided into elastic and plastic components, and the elastic components follow

$$\mathring{\boldsymbol{T}} = \boldsymbol{E}\boldsymbol{D}^e,\ \boldsymbol{D} = \boldsymbol{D}^e + \boldsymbol{D}^p,\ \mathring{\boldsymbol{T}} = \boldsymbol{E}\boldsymbol{D} - \Lambda \boldsymbol{E} - \frac{\partial f}{\partial \boldsymbol{T}'} \tag{34}$$

Then by substituting Eqs. (23), (26), (30), (31), (33) and (34) into Eq. (11), we can obtain another expression for the following positive valuable, namely, $\Lambda (\Lambda = \lambda)$:

$$\Lambda = \frac{\dfrac{\partial f}{\partial'} \boldsymbol{E}\boldsymbol{D}}{\dfrac{\partial f}{\partial \boldsymbol{T}'} \boldsymbol{E} \dfrac{\partial f}{\partial \boldsymbol{T}'} + J \dfrac{\mathrm{MD}}{(\mathrm{M}^2 - \zeta^2 + \eta^{*2})p'} (\mathrm{M}_s^2 - \eta^2)} \tag{35}$$

The loading criteria are given in the same way as those in the work by Asaoka et al. (1994, 2002) shown below:

$$\begin{cases} \Lambda > 0 & loading \\ \Lambda = 0 & neutral \\ \Lambda < 0 & unloading \end{cases} \quad (36)$$

In most cases, the denominator is positive, therefore, $\Lambda > 0$ is equivalent to the following relation:

$$\frac{\partial f}{\partial \boldsymbol{T}'} \cdot \boldsymbol{ED} > 0 \quad (37)$$

which is the same as the way proposed by Hashiguchi (1989, 1993), or Zienkiewicz and Taylor (1991). It should be pointed out that by adopting subloading concept, plastic strain may occur in the area within the normal yielding surface according to the above loading criteria, which is different from classical plastic models.

## PERFORMANCE OF THE PROPOSED MODEL

Nine parameters are involved in the proposed model, among which five parameters, M, N, $\tilde{\lambda}$, $\tilde{\kappa}$, and $\nu$ are the same as in the Cam-clay model. The other three parameters are listed below.

$a$ : parameters which controls the collapse rate of structure when the soil is subjected to shearing or compression

$m$: parameters which controls the losing rate of overconsolidation when the soil subjected to shearing or compression

$b_r$: parameters which controls the developing rate of stress-induced anisotropy when the soil subjected to shearing or compression

These three parameters have clear physical meanings and can be easily determined. In particular, the first two parameters are exactly the same as those in the model proposed by Asaoka et al. (2002). Therefore the method to determine them is also the same. Parameter br can be determined based on the performance of the soil which is influenced by the development of the stress-induced anisotropy when the soil is subjected to shearing or compression. By showing some performances of the model for different soils under different loading conditions, the reader can soon understand the physical meanings.

### *Influence of Overconsolidation When the Structure is Considered*

We now consider a set of sands with different densities similar to the work by Nakai (2005), which is prepared from a sand whose material parameters and initial condition are listed in Table 1 and 2. From the reference values for $R_r$, $R_r^*$, and $\zeta_r$, it is understood that the sand is originally a normally consolidated highly structured loose sand without stress-induced anisotropy and with a very large void ratio. The set of sands with different densities are just prepared by vibration compaction with different numbers of compactions, as shown in Fig. 5. The amplitude of the vibration is 2.3 kPa. After the compaction, these sands with different densities are then isotropically consolidated to a prescribed confining pressure of 294 kPa. Table 3 lists the initial values for these sands before they are subjected to cyclic loading under undrained condition. All these sands have the same five parameters which are listed in the upper part of Table 1.

**Table 1. Material parameters of sand**

| | |
|---|---|
| Compression index $\tilde{\lambda}$ | 0.050 |
| Swelling index $\tilde{\kappa}$ | 0.012 |
| Critical state parameter **M** | 1.0 |
| Void ratio **N** ($p' = 98$ kPa on N.C.L.) | 0.98 |
| Poisson's ratio $\nu$ | 0.30 |
| Degradation parameter of overconsolidation state $\boldsymbol{m}$ | 0.10 |
| Degradation parameter of structure $\boldsymbol{a}$ | 2.2 |
| Evolution parameter of anisotropy $\boldsymbol{b_r}$ | 1.5 |

**Table 2. Reference conditions of sand before vibrating compaction**

| | |
|---|---|
| Reference void ratio $\boldsymbol{e_r}$ | 1.29 |
| Reference mean effective stress $p'_r$ (kPa) | 10.0 |
| Reference degree of structure $\boldsymbol{R_r^*}$ | 0.00625 |
| Reference degree of overconsolidation $\boldsymbol{1/R_r}$ | 1.00 |
| Reference anisotropy $\xi_r$ | 0.00 |

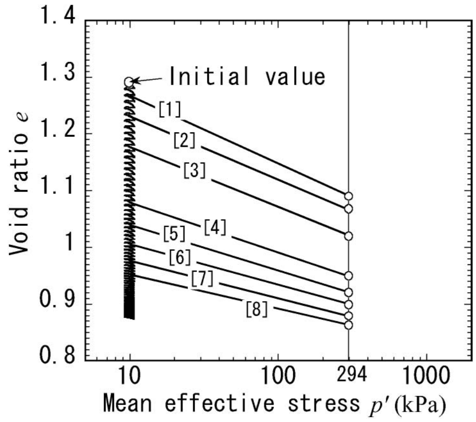


**Fig. 5. Set of sands with different densities prepared from a loose sand by vibration compaction**

Figure 6 shows the mechanical behavior of the set of sands with different densities in undrained cyclic compression tests. It is clear from the figure that very loose sand will fail along the way towards the zero effective stress state (the effective stress path) before cyclic mobility has a chance to occur. For medium dense sand, however, cyclic mobility does occur. Dense sand will never show cyclic mobility. Figure 7 shows the mechanical behavior of the set of sands with different densities in undrained triaxial compression tests. We believe that these results are very familiar to our readers who are interested in soil mechanics. The above results mean that the mechanical behavior of sand, subjected to monotonic/cyclic loading under undrained conditions, can be uniquely and correctly described by the proposed model no matter what density it may have.

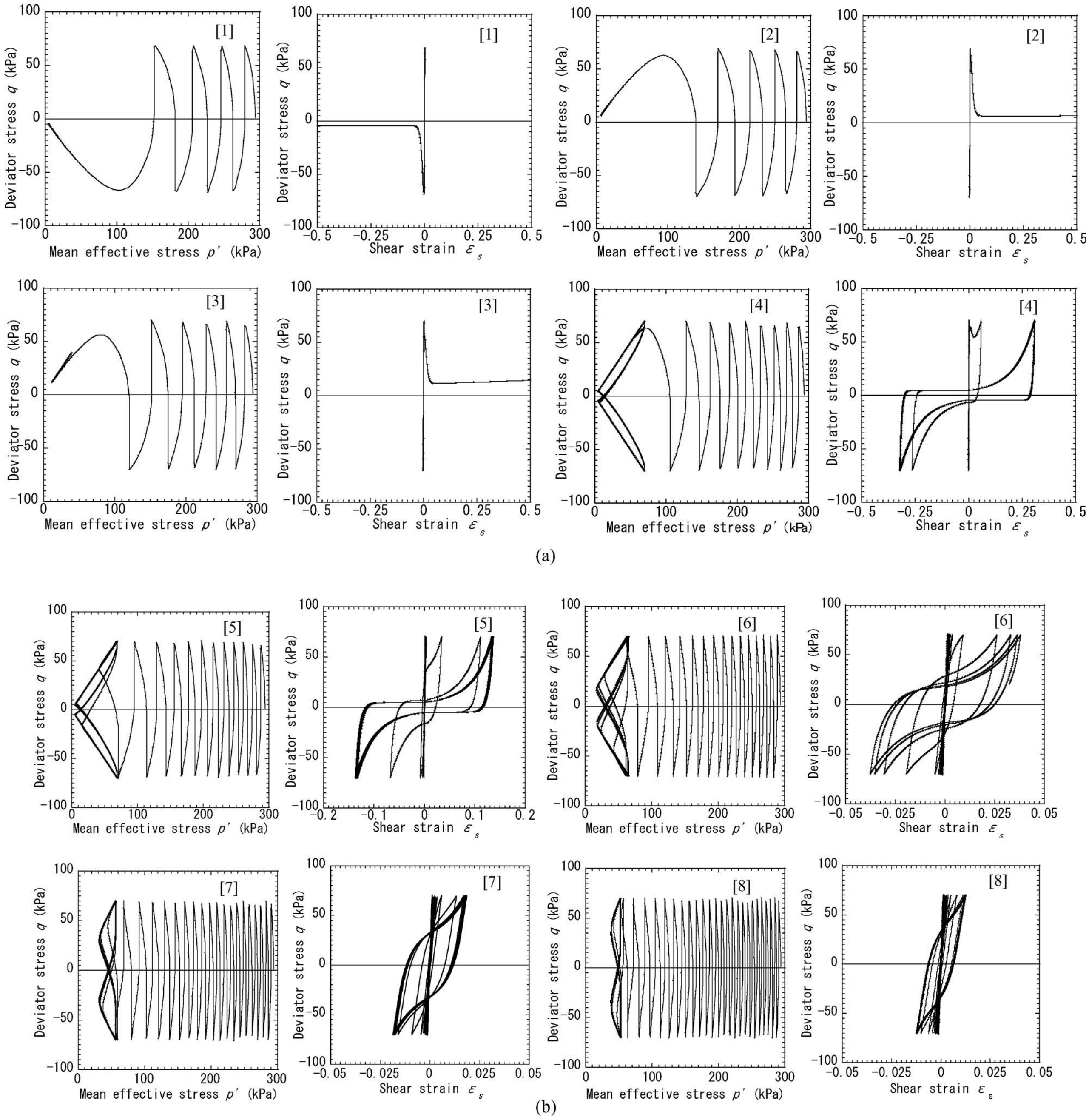


**Fig. 6. Mechanical behavior of the set of sands with different densities subjected to cyclic triaxial shear tests under undrained conditions**

*Influence of Overconsolidation When the Structure is not Considered*

In order to identify the influence of both overconsolidation and the structure, we prepared the same set of sands as in the previous section, but without considering the structure. Four of the sands listed in Table 3, namely, sands [1], [2], [5], and [8], are considered. The only difference is that structure $R^*$ is supposed to be 1.0 (no structure) for all four sands. In this case, however, it should be noted that these four sands have not originated from the unique loose sand listed in Tables 1 ~ 3 and Fig. 5. They are different sands.

Figure 8 shows the behavior of the set of sands with different densities in undrained cyclic compression tests. Comparing the results here with those in Fig. 6, in which the structure is considered, it is clear that loose sand liquefies with cyclic mobility, which is totally different from the simulated results in which the structure is considered. This implies that when the structure is not considered, it is impossible to describe the liquefaction behavior of loose sand. For dense sand, however, the structure does not affect the behavior of the sand in the cyclic mobility region, because the structure will soon collapse after being subjected to cyclic loading.

Another important thing that was observed in shaking table tests (Ye et al., 2006), and should be pointed out, is the phenomenon that after the excessive pore water pressure dissipates, the once-liquefied soils that are usually

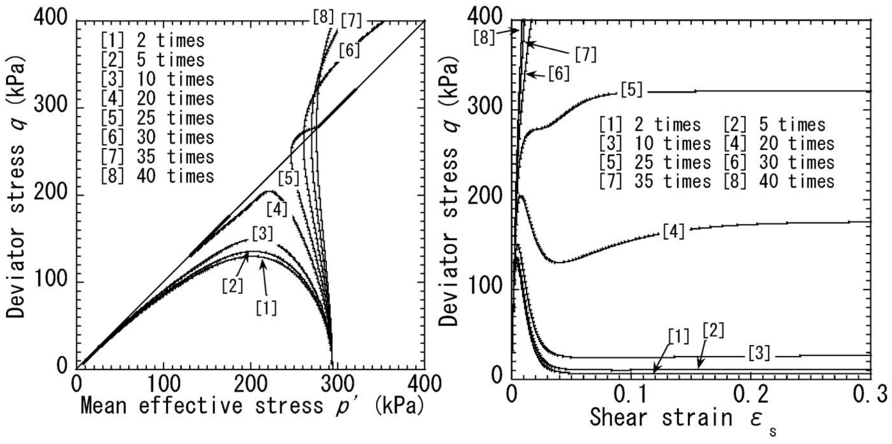


**Fig. 7. Mechanical behavior of the set of sands with different densities in undrained triaxial compression tests**

**Table 3. Initial conditions of sand before cyclic loading**

| | Vibration numbers $n$ | Initial void ratio $e_0$ | Initial degree of structure $R_0^*$ | Initial degree of overconsolidaiton $1/R_0$ | Initial anisotropy $\xi_0$ |
|---|---|---|---|---|---|
| [1] | 2 | 1.09 | 0.00950 | 1.19 | 1.5e-5 |
| [2] | 5 | 1.07 | 0.0160 | 1.51 | 1.6e-5 |
| [3] | 10 | 1.02 | 0.037 | 2.12 | 1.8e-5 |
| [4] | 20 | 0.947 | 0.150 | 3.73 | 2.6e-5 |
| [5] | 25 | 0.920 | 0.241 | 4.79 | 4.6e-5 |
| [6] | 30 | 0.897 | 0.341 | 6.07 | 1.1e-4 |
| [7] | 35 | 0.879 | 0.434 | 7.60 | 3.1e-4 |
| [8] | 40 | 0.865 | 0.516 | 9.40 | 8.1e-4 |

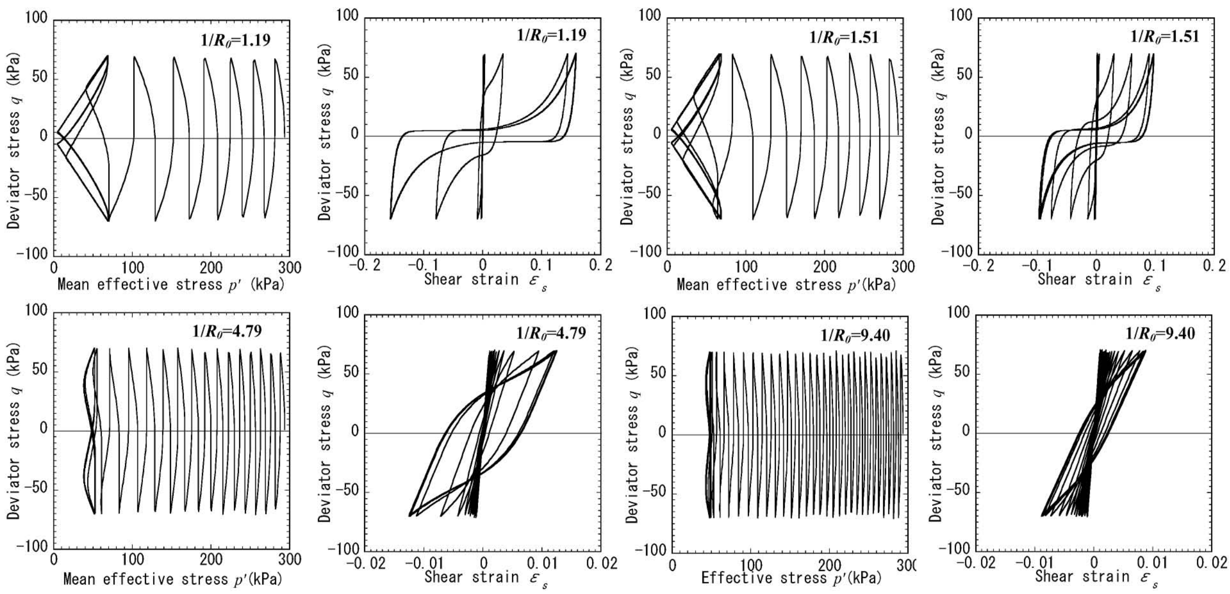


**Fig. 8. Mechanical behavior of the set of sands with different densities without considering the structure (undrained tests)**

thought to be denser than in their original state may liquefy again if subjected to strong motions. The present model can describe this phenomenon naturally based on the results shown in Fig. 8. Because it is clear from the figure that the liquefaction of the sand is not dependent on the structure of soil (The structure of soil only affects

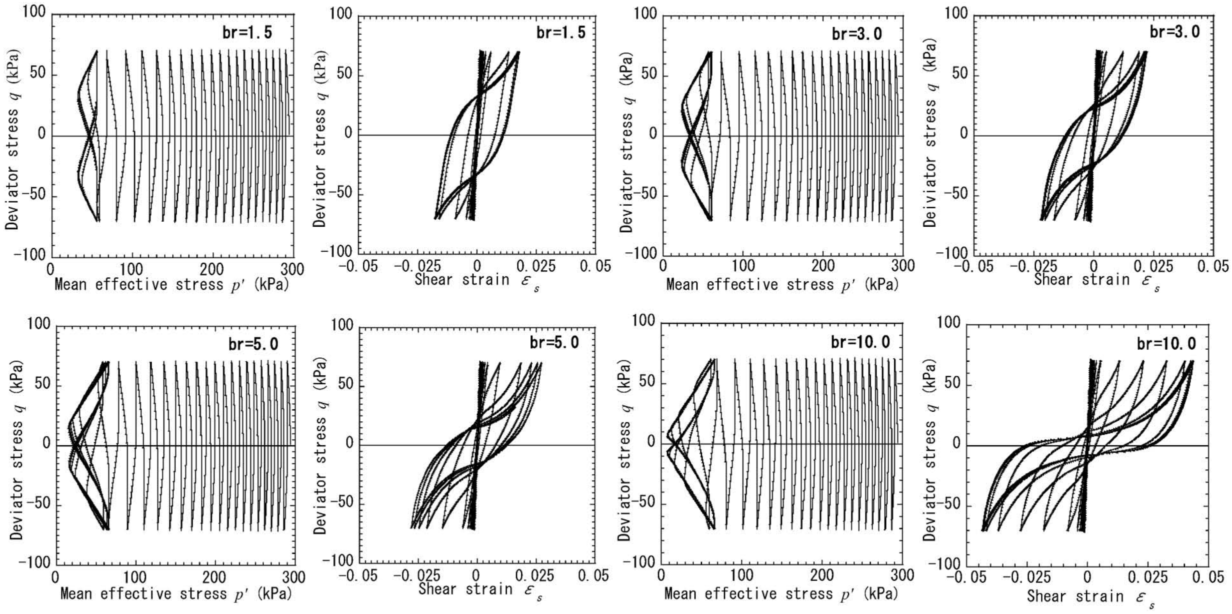


**Fig. 9. Influence of stress-induced anisotropy on the cyclic mobility of sand subjected to cyclic triaxial shear loading under undrained conditions**

the style of liquefaction in loose condition), it is only dependent on its density. Liquefied soils may get denser after dissipation of pore water pressure but may again liquefy if the density is not dense enough.

*Influence of Stress-induced Anisotropy*

In order to investigate the influence of stress-induced anisotropy on the mechanical behavior of rather dense sand, we prepared a set of sands whose material parameters and initial conditions are almost the same as those above, except for parameter $b_r$, which controls the developing rate of the stress-induced anisotropy. The sands considered here are altered versions of the sand marked by [7] in Fig. 5 and Table 3, namely, a rather dense sand. Figure 9 shows the degrees of cyclic mobility for these sands subjected to cyclic loading under undrained conditions. It is seen from the figure that the faster the development of the stress-induced anisotropy, the easier the stress path will run into the cyclic mobility region, that is, the easier it will be liquefied.

*Difference between Clayey Soils and Sandy Soils*

In the works by Asaoka et al. (2000a), it is pointed out that the difference between clayey soils and sandy soils depends on two factors, namely, the rate of loss in overconsolidation and the rate of the collapse of the structure during static shearing. For sandy soils, the rate of loss in overconsolidation is very slow, while the rate of the collapse of the structure is very fast. On the contrary, for clayey soils, the rate of loss in overconsolidation is very fast, while the rate of the collapse of the structure is very slow. Under cyclic loading conditions, however, it is necessary to confirm whether this conclusion still remains valid. A set of soils with the same initial conditions but different values for $a$ and $m$, which control the changing rates of overconsolidation and the collapse of the structure, are investigated for their behavior when subjected to cyclic loading under undrained conditions. Tables 4 and 5 list the material parameters and the initial conditions, respectively, for $a$ and $m$. They are changed to investigate their influence.

**Table 4. Material parameters of soils (from sandy soils to clayey soils)**

| | |
|---|---|
| Compression index $\tilde{\lambda}$ | 0.20 |
| Swelling index $\tilde{\kappa}$ | 0.065 |
| Critical state constant **M** | 1.0 |
| Void ratio **N** ($p'=98$ kPa on N.C.L.) | 0.98 |
| Poisson's ratio $\nu$ | 0.30 |
| Degradation parameter of overconsolidation $\boldsymbol{m}$ | 0.10 ~ 1.0 |
| Degradation parameter of structure $\boldsymbol{a}$ | 3.0 ~ 0.10 |
| Evolution parameter of anisotropy $\boldsymbol{b_r}$ | 1.5 |

**Table 5. Initial conditions of soils (from sandy soils to clayey soils)**

| | |
|---|---|
| Initial void ratio $\boldsymbol{e_0}$ | 0.76 |
| Initial mean effective stress $\boldsymbol{p'}$ (kPa) | 294 |
| Initial degree of structure $\boldsymbol{R_0^*}$ | 0.50 |
| Initial degree of overconsolidation $1/\boldsymbol{R_0}$ | 2.0 |
| Initial anisotropy $\xi_0$ | 0.00 |

Figure 10 shows the different types of behavior for sandy soils and clayey soils subjected to cyclic loading under undrained conditions. From this figure, it is very clear that by changing parameters $a$ and $m$, the difference between sandy soils and clayey soils can be easily and uniquely identified. For instance, in the case of $m=0.1$ and $a=3.0$, which means that the loss of overconsolidation is very slow while the collapse of the structure is very fast, a typical cyclic mobility behavior is observed. In the case of $m=1.0$ and $a=0.1$, however, which means that the loss of overconsolidation is very fast while the col-

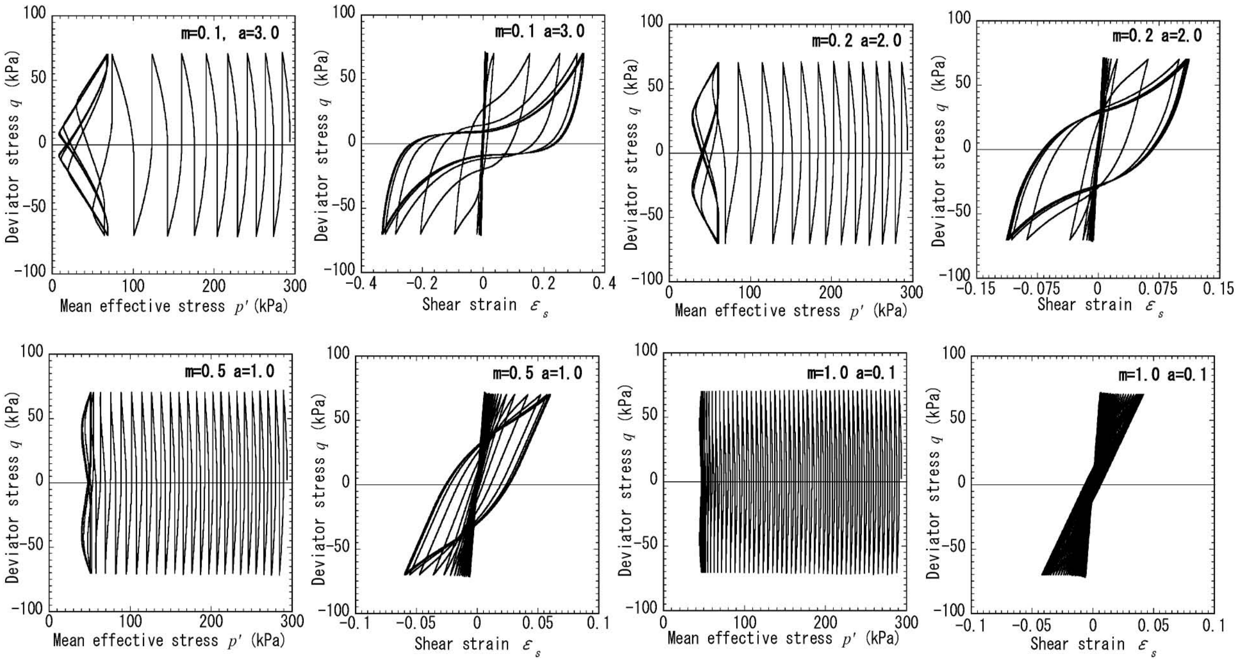


**Fig. 10. Different types of behavior for sandy soils and clayey soils subjected to cyclic triaxial shear loading under undrained conditions**

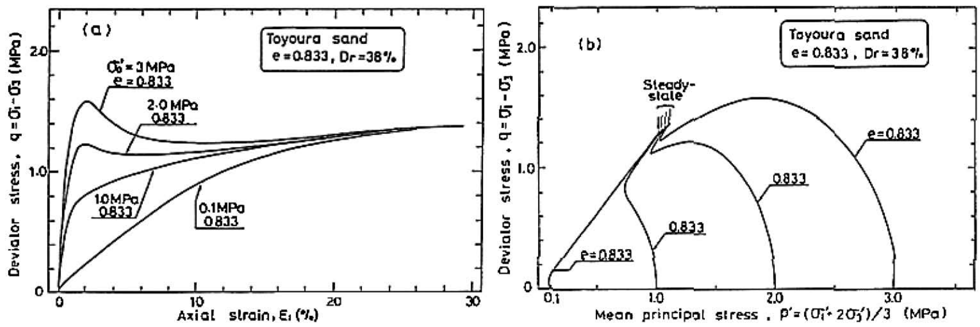


**Fig. 11. Test results for the confining-stress dependency of sand (after Ishihara, 1993)**

lapse of the structure is very slow, a typical clayey soil behavior under cyclic loading is observed. From the above discussion, it is very easy to explain why clay does not liquefy, namely, it is just that the structure of clay collapses very slowly so as to resist cyclic shearing. Unfortunately for sand, however, its structure collapses so fast that it liquefies easily if the density is loose enough. A similar conclusion can also be found in the work by Noda et al. (2004).

*Confining-stress Dependency of Sand in Undrained Monotonic Loading Tests*

Ishihara (1993) reported his experimental results in which four sands, with the same void ratios but under different confining pressures, were tested under undrained triaxial compression. The test results are given in Fig. 11. They show the phenomenon whereby if the confining stress is large, the sand behaves like loose sand, while if the confining stress is small, the sand behaves like dense sand. Such a phenomenon is called ''the confining-stress dependency of sand''. Similar test results to those shown in Fig. 12 can be found in the work by Nakai (2005), in which silica sand was used as the test material.

The present model can also describe this behavior properly. Figure 13 shows the simulated results that, on the whole, coincide well with the test results. In the simulation, the material parameters of the sand are the same as those listed in Table 1.

*Mechanical Behaviors of Sand under Drained Loading Test*

Only undrained loading problems have been discussed in the previous sections. The behavior of sand under drained conditions should also be discussed. We prepared the same set of sands as in the previous section. The four sands listed in Table 3, namely, sands [1], [5], [6], and [8], are considered. Figure 14 shows the stress-strain-dilatancy relations of the sands in drained triaxial compression tests.

Finally, it should be pointed out that all the theoretical

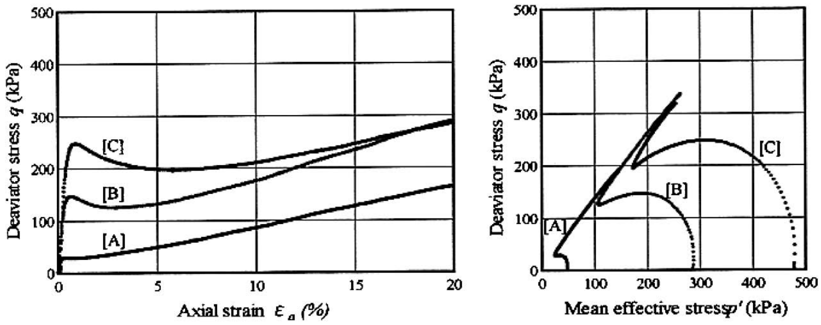


**Fig. 12. Test results for the confining-stress dependency of silica sand (after Nakai, 2005)**

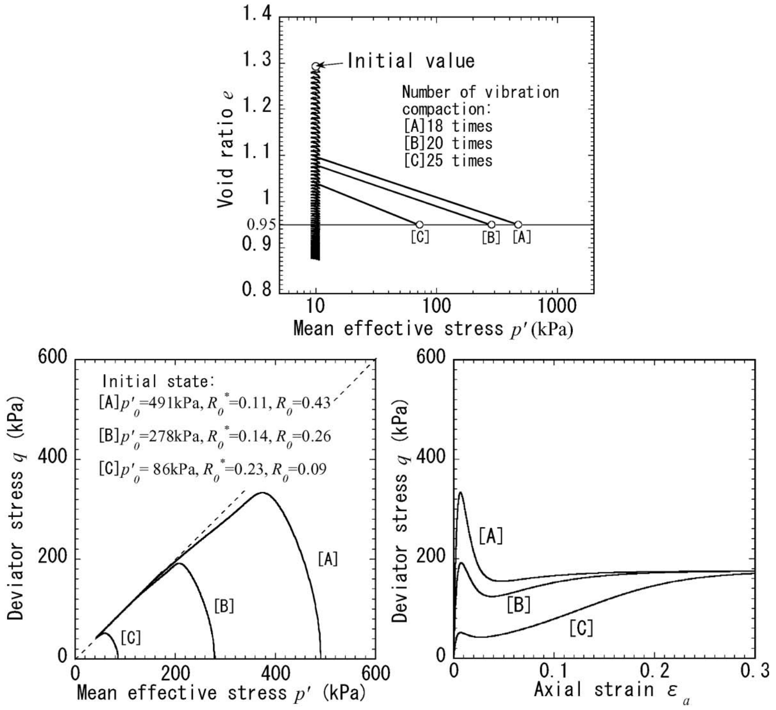


**Fig. 13. Simulation of the mechanical behavior of the set of sands with the same void ratios, but under different confining pressures, subjected to triaxial compression under undrained conditions**

simulations for the types of soil behavior discussed throughout this paper are conducted under triaxial conditions with a special loading path. Under generalized stress paths, however, further research should be conducted, e.g., to incorporate the $t_{ij}$ concept developed by Nakai and Mihara (1984), Nakai and Matsuoka (1986), Nakai (1989), and Nakai and Hinokio (2004), into the model proposed in this paper.

## CONCLUSIONS

In this paper, the authors proposed a new approach using the concept of stress-induced anisotropy to describe the cyclic mobility of soils. Since the proposed constitutive model is based on the model, proposed by Asaoka et al. (2002), most of the performance of the model remains alive. On the other hand, by introducing the new concept of stress-induced anisotropy and a new evolution equation for overconsolidation, it is possible to describe not only the mechanical behavior of soils under monotonic loading, but also the behavior of soils under cyclic loading. The following conclusions can be made:

1. The proposed model does not require any additional parameters. It has nine parameters, among which five are the same as those in the Cam-clay model and are familiar to most geotechnical researchers. The other three parameters, namely, $a$, $m$, and $b_r$, are the parameters that control the collapse rate of the structure, the losing rate of overconsolidation and the developing rate of the stress-induced anisotropy, respectively. The physical meanings for these parameters are clear and can be easily determined. The ninth parameter $b_l$, is introduced to express physically the limitation on the development of anisotropy that will not exceed C.S.L. ($\zeta < M$). Its value may vary from 0.90 to 0.99 according to the ex-

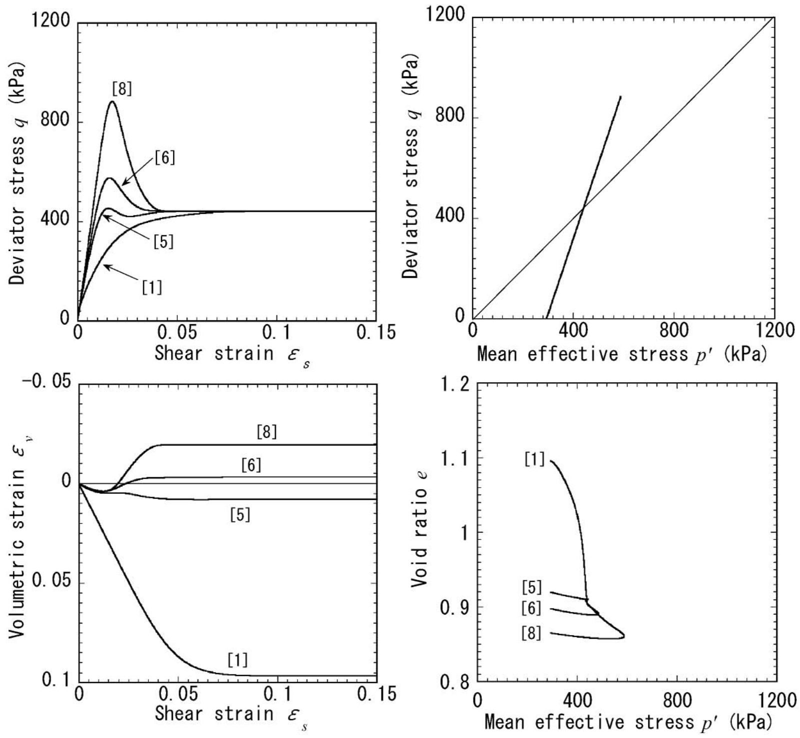


**Fig. 14. Stress-strain-dilatancy relations of the set of sands in drained triaxial compression tests**

planation of the ''completely liquefaction'' in engineering sense. The closer the value of $b_l$ is to 1.0, the closer the effective mean stress will be to zero in cyclic mobility region. Without losing generality, we fixed the value of $b_l$ at 0.95 throughout this paper. The limitation for the development of anisotropy is the same as the gradient of the C.S.L., namely, the anisotropic stress will never surpass the C.S.L. since limitation $\zeta < \mathrm{M}$ is sufficient. It is no longer necessary to have any other limitations.

2. The Critical State Line (C.S.L.), as the threshold between plastic compression and plastic expansion, proposed in the present model, is fixed, no matter what kind of effective stress path there may be, which makes the model look much more efficient, more realistic, and easier to handle.
3. The liquefaction of sand may consist of two types, that is, liquefaction without cyclic mobility in the case of loose sand and liquefaction with cyclic mobility in the case of medium dense sand. For loose sand, liquefaction is mainly caused by a quick collapse of the structure during shearing. For medium dense sand, however, liquefaction with cyclic mobility is mainly caused by the development of stress-induced anisotropy. For dense sand, liquefaction will not occur. All these types of behavior are described with a set of the same parameters. It is not necessary to assign, in advance, which sand will be liquefied or not. It is simply dependent on the state, namely, the overconsolidation ratio, the anisotropy, and the structure, once the material parameters have been fixed, in other words, once the sand has been selected.
4. In the works by Asaoka et al. (2002), it is stated that the difference in mechanical behavior between sands and clays is just the difference in the rates of the collapse of the structure and the loss of overconsolidation which happened to the soils when they were subjected to shearing. This statement is also valid for the cyclic mobility of soils subjected to cyclic loading under undrained conditions. That is, for clayey soils, the structure collapses very slowly while the overconsolidation declines easily. For sands, however, the structure collapses very quickly while the overconsolidation declines very slowly. Under some circumstances, the overconsolidation may even increase during plastic shearing, which is different from the assumption adopted in the model proposed by Asaoka et al. (2002) whereby the accumulation of overconsolidation only happens during the elastic unloading process. In a word, the mechanical behavior of soils subjected to cyclic loading under undrained conditions, can be uniquely described by the proposed model, no matter what kind of soil it may be.
5. The present model can describe the phenomenon whereby liquefied soils may liquefy again if they are subjected to strong motions after the excessive pore water pressure has dissipated.
6. The rate of the development of the stress-induced anisotropy affects the degree of the cyclic mobility of sandy soils. The faster the rate, the more likely the cyclic mobility of soils may occur.

## ACKNOWLEDGEMENTS

The authors wish to express their sincere thanks to Professor Akira ASAOKA of Nagoya University and Professor Teruo NAKAI of Nagoya Institute of Technology, for their valuable comments. The second author also wishes to express his thanks to Professor Atsushi YASHIMA of Gifu University for his kindness in providing a good environment for the author's graduate research activities.

## REFERENCES

1) Asaoka, A., Nakano, M. and Noda, T. (1994): Soil-water coupled behavior of saturated clay near/at critical state, *Soils and Foundations*, **37** (1), 91–105.
2) Asaoka, A., Nakano, M. and Noda, T. (1998): Super loading yield surface concept for the saturated structured soils, *Proc. 4th European Conference on Numerical Methods in Geotechnical Engineering-NUMGE98*, 232–242.
3) Asaoka, A., Nakano, M. and Noda, T. (2000a): Superloading yield surface concept for highly structured soil behavior, *Soils and Foundations*, **40** (2), 99–110.
4) Asaoka. A., Nakano, M., Noda, T. and Kaneda, K. (2000b): Delayed compression/consolidation of naturally clay due to degradation of soil structure, *Soils and Foundations*, **40** (3), 75–85.
5) Asaoka, A., Noda, T., Yamada, E., Kaneda, K. and Nakano, M. (2002): An elasto-plastic description of two distinct volume change mechanisms of soils, *Soils and Foundations*, **42** (5), 47–57.
6) Green, A. E. and Naghdi, P. M. (1965): A general theory of an elastic-plastic continuum, *Archive for Rational Mechanics and Analysis*, **18**, 251–281.
7) Hashiguchi, K. and Ueno, M. (1977): Elastoplastic constitutive laws of granular material, Constitutive Equations of Soils, *Proc. 9th ICSMFE.*, Spec. Ses. 9 (eds. by Murayama, S. and Schofield, A. N.), Tokyo, JSSMFE, 73–82.
8) Hashiguchi, K. (1978): Plastic constitutive equations of granular materials, *Proc. US-Japan Seminar on Continuum Mechanics and Statistical Approaches in the Mechanics of Granular-Materials* (eds. by Cowin, S. C. and Satake, M.), Sendai, JSSMFE, 321–329.
9) Hashiguchi, K. (1989): Subloading surface model in unconventional plasticity, *Int. J. of Solids and Structures*, **25**, 917–945.
10) Hashiguchi, K. (1993): Fundamental requirements and formulation of elasto-plastic constitutive equations with tangential plasticity, *International Journal of Plasticity*, **9**, 525–549.
11) Hashiguchi, K. and Chen, Z. P. (1998): Elasto-plastic constitutive equations of soils with the subloading surface and the rotational hardening, *Int. J. Numer. Anal. Meth. And Geomech.*, **22**, 197–227.
12) Hinokio, M. (2000): Deformation characteristic of sand subjected to monotonic and cyclic loadings and its application to bearing capacity problem, *Doctoral Thesis*, Nagoya Institute of Technology, 141–144 (in Japanese).
13) Hyodo, M., Tanimizu, H., Yasufuku, N. and Murata, H. (1994): Undrained cyclic and monotonic triaxial behavior of saturated loose sand, *Soils and Foundations*, **34** (1), 19–32.
14) Ishihara, K. (1993): Liquefaction and flow failure during earthquake, The 33rd Rankine Lecture, *Geotechnique*.
15) Kato, S., Ishihara, K. and Towhata, I. (2001): Undrained shear characteristics of saturated sand under anisotropic consolidation, *Soils and Foundations*, **41** (1), 1–11.
16) Nakai, T. and Mihara, Y. (1984): A new mechanical quantity for soils and its application to elastoplastic constitutive models, *Soils and Foundations*, **24** (2), 82–94.
17) Nakai, T. and Matsuoka, H. (1986): A generalized elastoplastic constitutive model for clay in a three-dimensional stresses, *Soils and Foundations*, **26** (3), 81–89.
18) Nakai, T. (1989): An isotropic hardening elastoplastic model for sand considering the stress path dependency in three-dimensional stresses, *Soils and Foundations*, **29** (1), 119–137.
19) Nakai, T. and Hinokio, M. (2004): A simple elastoplastic model for normally and over consolidated soils with unified material parameters, *Soils and Foundations*, **44** (2), 53–70.
20) Nakai, K. (2005): An elasto-plastic constitutive modeling of soils based on the evolution laws describing collapse of soil skeleton structure, loss of overconsolidation and development of anisotropy, *Doctoral Thesis*, Nagoya University (in Japanese).
21) Noda, T., Nakano, M. and Asaoka, A. (2004): Mechanical differences between sand and clay under monotonic and cyclic loading, *Proc. Int. Conference on Cyclic Behavior of Soils and Liquefaction Phenomena (CBS04)*, Bochum, Germany, March 31- April 02, 77–84
22) Oka, F. (1992): A cyclic elasto-viscoplastic constitutive model for clay based on the non-linear hardening rule, *Proc. 4th International Symposium on Numerical Models in Geomechanics*, Swansea, 105–114.
23) Oka, F., Yashima, A., Kato, M. and Sekiguchi, K. (1992): A constitutive model for sand based on the non-linear kinematic hardening rule and its application, *Proc. 10th World Conf. Earthquake Engineering*, Madrid, **5**, Balkema, 2529–2534.
24) Oka, F., Yashima, A., Shibata, T., Kato, M. and Uzuoka, R. (1994) FEM-FDM coupled liquefaction analysis of a porous soil using an elasto-plastic model, *Applied Scientific Research*, **52**, 209–245.
25) Oka, F., Yashima, A., Tateishi, A., Taguchi, Y. and Yamashita, S. (1999): A cyclic elastoplastic constitutive model for sand considering a plastic-strain dependence of the shear modulus, *Geotechnique*, **49** (5), 661–680.
26) Roscoe, K. H., Schofield, A. N. and Thurairajah, A. (1963): Yielding of clays in states wetter than critical, *Geotechnique*, **13** (3), 250–255.
27) Schofield, A.N. and Wroth, C. P. (1968): *Critical State Soil Mechanics*, McGraw-Hill.
28) Sekiguchi, H. (1977): Rheological characteristics of clays, *Proc. 9th ICSMFE.*, Tokyo, **1**, 289–292.
29) Yashima, A., Oka, F., Shibata, T. and Uzuoka, R. (1991): Liquefaction analysis by LIQCA, *Proc. JGS Conference on Liquefaction of Ground and its Counter Measure*, 165–174 (in Japanese).
30) Ye, B., Yokawa, H., Kondo, T., Yashima, A., Zhang, F. and Yamada, H. (2006): Investigation on stiffness recovery of liquefied sandy ground after liquefaction using shaking-table tests, Test, soil and rock behavior and modeling, *ASCE Geotechnical Special Publication*, (150), 482–489.
31) Zienkiewicz, O. C. and Taylor, R. L. (1991): *The Finite Element Method,* **2**, 4th ed., McGraw-Hill.